Instrument and method for measuring second-order nonlinear optical tensors

Darrell J. Armstrong, Michael V. Pack, and Arlee V. Smith[a]

Department 1118, Sandia National Laboratories, Albuquerque, New Mexico 87185-1423

We describe an apparatus for measuring the second-order nonlinear tensor of crystals based on the measurement technique of separated-beam, nonphase matched, second-harmonic generation. This method is an improvement over traditional methods based on the analysis of Maker fringes. We illustrate our measurement technique and show some typical data for crystals of potassium dihydrogen phosphate and potassium niobate. We intend to maintain our apparatus to encourage rapid and complete characterization of new nonlinear crystals, and also to improve the nonlinear tensor data base for established nonlinear crystals. © *2003 American Institute of Physics.*
[DOI: 10.1063/1.1581393]

I. INTRODUCTION

Although second harmonic generation and other nonlinear processes have been studied extensively since the first demonstration of frequency doubling by Franken *et al.*[1] in 1962, the uncertainties in the values of the second-order susceptibilities of commonly used nonlinear crystals are often ±20% or more. Part of the reason for this dearth of precise information is the fact that the standard Maker fringe measurement methods are difficult to apply. In this article we describe the separated-beams method[2] which we find easier to apply, along with a description of the laboratory apparatus we have developed. Encouraged by our success in measuring the full nonlinear tensor of several commonly used crystals, we plan to keep the apparatus permanently operational so that as new crystals are developed they can be quickly characterized, and also to continue improving the characterization of existing crystals.

Methods of measuring the nonlinear optical tensor, *d*, of crystals based on second harmonic generation can be categorized as either phase matched or nonphase matched. For a fixed fundamental wavelength, phase matching is achievable only for a limited set of propagation angles. This set is usually too restricted to allow the determination of the entire nonlinear tensor. In contrast, nonphase matched methods permit any propagation direction, making the entire nonlinear tensor accessible to measurement.

Nonphase matched measurements of crystal nonlinearity date back to a 1962 paper by Maker *et al.*[3] which reported the observation of a $\sin^2(\Delta k L/2)$ oscillation in the second harmonic power as the angle of a thin plate of crystalline quartz was rotated to vary the effective thickness, *L*. This variation with angle can be used to deduce $\Delta k = k_{2\omega} - 2k_\omega$ which, combined with a measurement of the input fundamental and output harmonic field strengths, allows the determination of the effective nonlinearity d_{eff}. This method has

been used successfully for 40 yr and is well developed. However, it poses several technical challenges. Among them are multiple reflections from the parallel input and output surfaces which can enhance the fundamental and the harmonic waves inside the crystal, leading to overestimations of d_{eff}. This problem is especially severe if the refractive index is high.[4–6] Antireflection coatings reduce this problem, but if the sample is tilted to large angles, changes in the coating reflectivity with angle must be considered. Another problem is that walkoff, or angular displacement of the fundamental and harmonic beams, can be significant if the beam diameters are small. There are two types of walkoff: birefringent walkoff and a tilt-dependent walkoff that is proportional to Δk.[7] Another issue complicating analysis is that the contributions of the various d_{ijk} elements to d_{eff} change with crystal angle, as does the value of Δk. Also, if the tilt angle becomes large, the beam profile inside the crystal changes from circular to elliptical.

The translated-wedge variation of the Maker fringe method[4,8,9] addresses most of these problems, but analysis can still be tedious. In this method the crystal is prepared with nonparallel surfaces. The wedge angle is chosen large enough that the étalon fringes from multiple reflections are closely spaced compared with the beam diameter. This minimizes but does not eliminate the effect of multiple reflections.[10] On the other hand, the wedge angle is chosen small enough that the variation of the crystal thickness across the beam diameter is much less than a coherence length. Maker fringes are mapped as the wedge is translated across the beam to vary the thickness over a range of many coherence lengths. The fringe period gives Δk, which is combined with the strength of the fundamental and harmonic beams to determine d_{eff}. The Maker fringes can be complex, with multiple overlapped fringes arising from different mixing processes. For example, the *e*-polarized harmonic can be driven by three combinations of polarizations for the two fundamental waves, *ee*, *eo*, and *oo*. Each process has a different value of Δk and thus a different fringe period. The individual contributions, including their relative signs, can be found by analyzing the fringes for different fundamental and

---

[a]Author to whom correspondence should be addressed; electronic mail: arlee.smith@osa.org
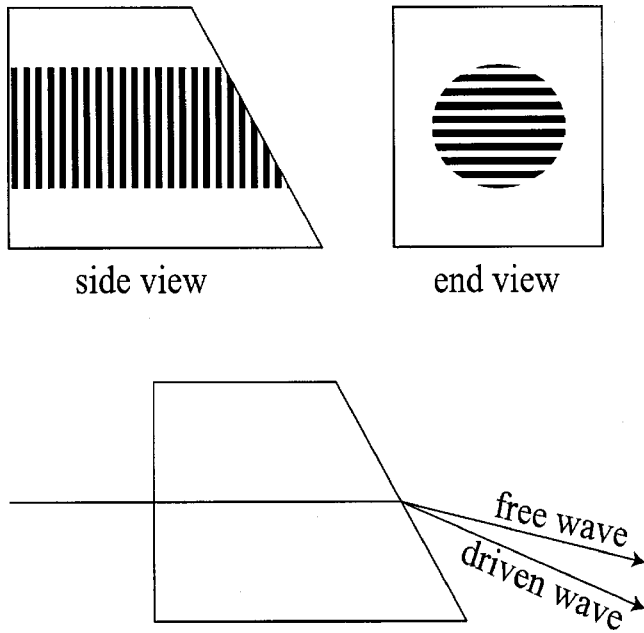
     3250   © 2003 American Institute of Physics

side view   end view

free wave

driven wave

FIG. 1. A crystal wedge is used for the separated-beams method of measuring d_{eff}. The alternating light and dark bands seen in the side view of the crystal represent zones of bright and dark second harmonic. They are spaced one coherence length apart. The exit face of the crystal is cut at a large enough angle to intersect several bands, as seen in the end view, assuring that in the far field there will be two well separated second harmonic beams: the free and driven waves.

harmonic polarizations. With the proper set of crystal cuts the entire nonlinear tensor can be measured, including the relative signs of all the elements.

The separated-beams method developed by Gehr and Smith[2] eliminates fringe analysis by using a crystal sample with a large wedge angle. The input face is normal to the input beam but the exit face is tilted at a large enough angle that the crystal thickness varies by several coherence lengths across the beam diameter as illustrated in Fig. 1. The modulation of the harmonic beam across the exit face implies that the beam is split into two separate beams in the far field: a free wave and a driven wave. The free wave can be thought of as a harmonic wave generated at the input face, which propagates as a normal or free harmonic wave thereafter. The refraction angle of the free wave is determined from Snell's law using as the crystal refractive index the value for the second harmonic wave, n_2. The driven wave is directly tied to the harmonic polarization, and thus to the fundamental wave. It can be thought of as being generated at the exit face, with its refraction angle determined by the refractive index of the fundamental wave, n_1. The Maker fringes of a parallel-faced sample are interferences between these two waves which are not spatially separated. In the separated-beams method, the emerging beams are not parallel so there is no interference between them and hence there are no fringes and no fringe analysis. Instead the value of Δk is found from the refractive indices of the fundamental and harmonic waves which in turn are found from the refraction angles of the free and driven waves.

II. THEORY OF THE SEPARATED-BEAMS METHOD

Because the boundary conditions that determine the strengths of the free and driven waves are simpler for the

free wave than for the driven wave, we use only the free wave whenever possible. Further, if the crystal is cut for propagation along one of the crystal axes x, y, or z, the individual d_{ijk} elements can be measured independently. Usually we use crystal samples cut along these three directions. Only the tensor elements with all three direction subscripts, d_{xyz}, d_{yxz}, and d_{zxy} require propagation along a different direction. To measure these we use propagation along one of the diagonal directions: $(x=y), (x=z)$, or $(y=z)$. Note that for these diagonal directions, there may be birefringent walkoff. We will discuss the birefringent corrections necessary for these cases later. First we consider the strengths of the free and driven waves for the case with no walkoff. These are set by boundary conditions at the faces of the crystal.[5,7,8,11] The driven wave is the specific solution to the wave equation which is given by Bloembergen and Pershan[11] as

$$E_d = \frac{-1}{\epsilon_0(n_2^2 - \bar{n}_1^2)}\left[P_{\text{NL}} - \frac{\bar{k}_1(\bar{k}_1 \cdot P_{\text{NL}})}{|k_2|^2}\right], \tag{1}$$

where P_{NL} is the nonlinear crystal polarization at the harmonic frequency, and n_2 is the refractive index of the harmonic wave. We always describe the fundamental as two waves: one unprimed and one primed. If two polarizations of the fundamental are involved, the partition of the fundamental is by polarization direction. If one polarization is involved, we divide the energy evenly between two identical waves. In Eq. (1), $\bar{n}_1$ is the mean of the refractive indices of the two driving fundamental waves: n_1 and n_1' and $\bar{k}_1 = k_1 + k_1'$. At the uncoated crystal input face the boundary condition is that the total tangential electric and magnetic fields must be continuous across the boundary. We must consider a weak reflected harmonic wave as well as the driven and free waves. The free and reflected fields are entirely tangential because we have chosen normal incidence, so the electric field equation is

$$E_r = E_f + E_d^t, \tag{2}$$

where E_f is the field of the free wave, E_r is the field of the reflected harmonic wave, and E_d^t is the tangential component of the driven wave. From Eq. (1) the tangential component of the driven wave is

$$E_d^t = \frac{-P_{\text{NL}}^t}{\epsilon_0(n_2^2 - \bar{n}_1^2)}, \tag{3}$$

where P_{NL}^t is the tangential component of the harmonic polarization given by

$$P_{\text{NL}}^t = \epsilon_0 d_{\text{eff}} E_1 E_1'. \tag{4}$$

Equating the tangential magnetic fields gives

$$-E_r = n_2 E_f + \bar{n}_1 E_d^t. \tag{5}$$

Combining these equations gives

$$E_f = -E_d^t\left[\frac{\bar{n}_1 + 1}{n_2 + 1}\right] = \left[\frac{\bar{n}_1 + 1}{n_2 + 1}\right]\frac{d_{\text{eff}} E_1 E_1'}{(n_2^2 - \bar{n}_1^2)}. \tag{6}$$
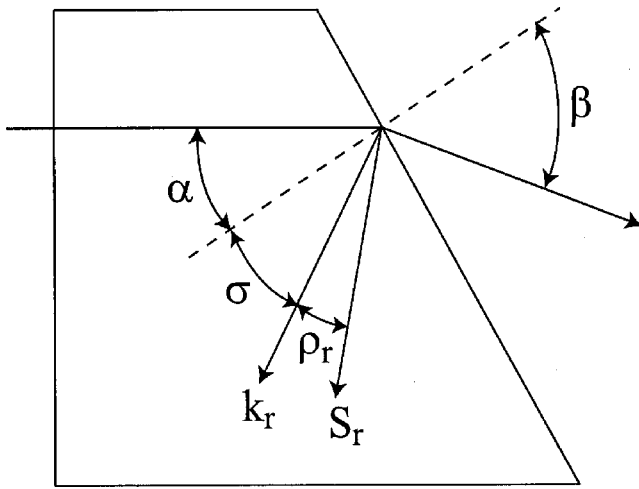
FIG. 2. Definitions of angles. For a p-polarized free wave the incident angle α and reflected angle σ are different. The reflected wave will have a birefringent walkoff angle ρ_r which is the angle between the reflected wave's propagation vector, k_r, and its Poynting vector, S_r.

The fundamental fields, E_1 and E_1', are those inside the crystal. They are related to the incident fields by

$$E_1 = E_1(\text{incident})t_1, \tag{7}$$

$$E_1' = E_1'(\text{incident})t_1', \tag{8}$$

where t_1 and t_1' are transmission coefficients for the fundamental waves at the input face. Similarly the free wave is that inside the crystal which is related to the emitted free wave by

$$E_f(\text{emitted}) = E_f t_2, \tag{9}$$

where t_2 is the transmission coefficient for a harmonic wave at the exit face. Written in terms of the *external* fields Eq. (6) becomes

$$E_f = \frac{d_{\text{eff}}}{(n_2^2 - \bar{n}_1^2)}\left[\frac{\bar{n}_1 + 1}{n_2 + 1}\right]E_1 E_1' t_1 t_1' t_2. \tag{10}$$

The transmission coefficients are given by

$$t_1 = \frac{2}{1 + n_1}, \tag{11}$$

$$t_1' = \frac{2}{1 + n_1'}. \tag{12}$$

When the free wave is s polarized at the exit face the transmission coefficient is given by

$$t_2 = \frac{2n_2\cos\alpha}{n_2\cos\alpha + \cos\beta}, \tag{13}$$

where the angles are shown in Fig. 2. For a p-polarized free wave the transmission coefficient is

$$t_2 = \frac{n_r\cos(\alpha)\cos\rho_r + n_2\cos(\sigma \pm |\rho_r|)}{n_r\cos\beta\cos\rho_r + \cos(\sigma \pm |\rho_r|)}, \tag{14}$$

where the reflected angle σ is found from

$$n_2\sin\alpha = n_r\sin\sigma \tag{15}$$

and ρ_r is the walkoff angle of the reflected wave with the positive sign used if birefringent walkoff increases the angle between the surface normal and the Poynting vector of the reflected wave.

For convenience we write the free wave energy as

$$U_f = Cd_{\text{eff}}^2 U_1 U_1' \mathcal{N}^2 \tag{16}$$

where U_1 is the fundamental pulse energy, and C is a constant determined by the fundamental beams' space and time profiles and $\mathcal{N}$ is a dimensionless number that depends only on the refractive indices and the exit face angle

$$\mathcal{N} = \frac{t_1 t_1' t_2}{(n_2^2 - \bar{n}_1^2)}\left[\frac{\bar{n}_1 + 1}{n_2 + 1}\right]\left[\frac{\cos\beta}{\cos\alpha}\right]^{1/2}$$

$$= \frac{2k_0 t_1 t_1' t_2}{\Delta k(n_2 + \bar{n}_1)}\left[\frac{\bar{n}_1 + 1}{n_2 + 1}\right]\left[\frac{\cos\beta}{\cos\alpha}\right]^{1/2}. \tag{17}$$

We have just described the behavior of a single mixing process, characterized by one set of fundamental and harmonic eigenpolarizations. However, there can be up to five separated beams in the far field: two free-wave beams, one for each harmonic eigenpolarization, which we will label $\mathcal{F}_i$ with the subscript indicating the polarization, and three driven-wave beams which we will label $\mathcal{D}_{ij}$ with the two subscripts corresponding to the polarizations of the two fundamental waves. For example, if a biaxial crystal is cut for propagation along the z axis, the two eigenpolarizations are x and y. The x- and y-polarized free waves are emitted at angles determined by $n_{2,x}$ and $n_{2,y}$. The driven waves are in general a mixture of x and y polarizations. However, their far field angles are determined by the fundamental refractive indices $n_{1,x}, (n_{1,x} + n_{1,y})/2$, and $n_{1,y}$ which we call $\bar{n}_1$.

Both of the free waves can have contributions from each of the three combinations of fundamental polarizations. In our example of a z-cut biaxial crystal, the x-polarized free wave can be driven by two x-polarized fundamental waves with nonlinear coefficient d_{xxx} and by an x- and a y-polarized fundamental wave with nonlinear coefficient d_{xxy}, and by two y-polarized fundamental waves with nonlinear coefficient d_{xyy}. These contributions add coherently so the general expression for energy in the x-polarized free wave is

$$\mathcal{F}_x = CU_1^2|d_{xxx}\mathcal{N}_{xxx}\cos^2\psi + d_{xyy}\mathcal{N}_{xyy}\sin^2$$

$$+ d_{xxy}\mathcal{N}_{xxy}\sin(2\psi)|^2, \tag{18}$$

where ψ is the polarization angle of the fundamental measured from the x axis, . The $\mathcal{N}_{ijk}$s were defined in Eq. (17).

In the laboratory the d_{ijk}s can be found relative to a reference crystal such as KDP by using the same fundamental beam which leaves C unchanged. For example, we can use a KDP crystal cut for propagation along the diagonal $(x=y)$. The z-polarized free wave energy will be

$$\mathcal{F}_x = CU_1^2|d_{xxy}\mathcal{N}_{xxy}\cos^2\psi|^2, \tag{19}$$

where ψ is the angle of the fundamental polarization relative to the xy plane.

The measurement can be made absolute instead of relative if we completely characterize the spatial and temporal properties of the fundamental beam, and calculate the value of C. For example, if the fundamental beam is Gaussian in space and time with form

TABLE I. Crystal cuts required for complete measurement of d with and without the assumption of Kleinman symmetry. The symbol ★ indicates a required crystal cut, (1 1 1) represents a choice of one of three cuts, (2 2 2) indicates two of three cuts.

Crystal class	Without Kleinman						With Kleinman					
	x	y	z	xy	xz	yz	x	y	z	xy	xz	yz
1	★	★	★	(2	2	2)	★	★	★	(1	1	1)
$2b\|\|\hat{y}$	★		★	(2	2	2)	★		★	(1	1	1)
$m(b\|\|\hat{y})$	★	★	★				★	★	★			
222				(2	2	2)				(1	1	1)
$mm2(x=\text{rot. axis})$		★	★					★	★			
4	(1	1)		(1	1)		(1	1)				
$\bar{4}$	(1	1)	★				(1	1)		★		
4mm	(1	1)					(1	1)				
$\bar{4}2m$				★						★		
3	★	★		(1	1)		★	★				
32		★		(1	1)			★				
3m	★						★					
6	(1	1)		(1	1)		(1	1)				
$\bar{6}$	★	★					★	★				
6mm	(1	1)					(1	1)				
$\bar{6}m2$	★						★					
23				(1	1	1)				(1	1	1)
$\bar{4}3m$				(1	1	1)				(1	1	1)

$$E_1 = E_0 e^{-t^2/\tau^2} e^{-r^2/R^2} \tag{20}$$

the constant C is given by[2]

$$C = \frac{2}{\pi^{3/2}\tau R^2 \epsilon_0 c}. \tag{21}$$

To measure the full d tensor it is often necessary to use several crystal cuts. We illustrate this for class m crystals which have d of the form

$$d = \begin{pmatrix} d_{xxx} & d_{xyy} & d_{xzz} & 0 & d_{xxz} & 0 \\ 0 & 0 & 0 & d_{yyz} & 0 & d_{yxy} \\ d_{zxx} & d_{zyy} & d_{zzz} & 0 & d_{zxz} & 0 \end{pmatrix}. \tag{22}$$

The x-polarized free wave is driven only by elements in the first row of d, and likewise y- or z-polarized free waves are driven only by elements in the second and third rows. Using a z-cut sample, the x-polarized free wave is driven by d_{xxx} and d_{xyy} with the form

$$\mathcal{F}_x = C U_1^2 |d_{xxx}\mathcal{N}_{xxx}\cos^2\psi + d_{xyy}\mathcal{N}_{xyy}\sin^2\psi|^2, \tag{23}$$

from which the relative magnitudes and signs of d_{xxx} and d_{xyy} can be determined by measuring the dependence of $\mathcal{F}_x$ on ψ, assuming the $\mathcal{N}_{ijk}$s are known. Using a y-cut crystal the x-polarized free wave is given by

$$\mathcal{F}_x = C U_1^2 |d_{xxx}\mathcal{N}_{xxx}\cos^2\psi + d_{xzz}\mathcal{N}_{xzz}\sin^2\psi$$
$$+ d_{xxz}\mathcal{N}_{xxz}\sin(2\psi)|^2 \tag{24}$$

from which the magnitudes and signs of d_{xzz} and d_{xxz} relative to d_{xxx} can be determined by varying ψ. Thus the relative values of all coefficients in the top row of d are measured.

In a similar fashion we can use x-cut and y-cut crystals to measure the relative values of all coefficients in the bottom row of d. We can then apply Kleinman symmetry to link the signs of the top and bottom rows. According to this approximate symmetry $d_{xxz}=d_{zxx}$ and $d_{xzz}=d_{zxz}$ so it is safe to assume that these pairs of coefficients have the same signs. Similarly the coefficients of the middle row of d are linked by Kleinman symmetry to elements of the top and bottom rows. The relative signs of all the tensor elements are now determined. Kleinman symmetry also links magnitudes, of course, but it may be desirable to measure them directly rather than relying on symmetry alone.

In Table I we show sets of crystal cuts that can be used for a complete determination of d for crystals of the various symmetry classes, both with and without the assumption of
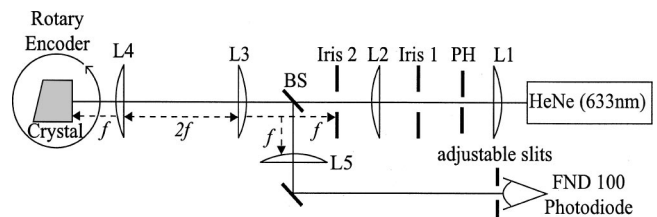

FIG. 3. Layout of the apparatus used to measure α, the exit face angle. $L1-L5$ are 2 in. diam achromatic lenses. Lenses $L3$ and $L4$ both have a focal length of f. PH is a pinhole.
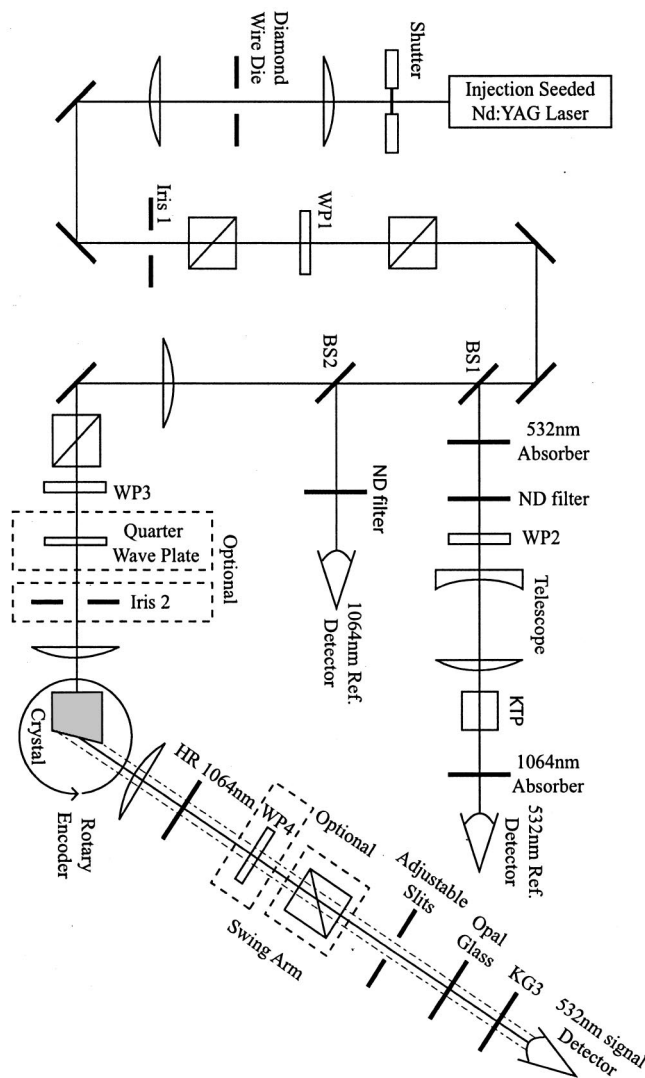
FIG. 4. Layout of the apparatus used to measure the beam angles, β, and the second harmonic pulse energies. WP1–WP3 are sapphire half-wave plates for 1064 nm.

Kleinman symmetry. For the uniaxial classes ($4-\bar{6}m2$) we avoid the z cut because it can be difficult to maintain polarization for propagation along the optic axis.

III. APPARATUS AND MEASUREMENT TECHNIQUES

The requirements of the laboratory measurements are to determine the $\mathcal{N}$s and the strengths of the free waves, perhaps relative to those generated by a reference crystal, as functions of the fundamental polarization angle ψ. The $\mathcal{N}$s are entirely determined from the crystal angle α and the refractive indices which are deduced from the directions of the free and driven waves. We will describe in detail each of these measurements starting with measurements of α.

A. Measurement of α

The exit face angle α is measured using the apparatus shown in Fig. 3. The beam from a He–Ne laser (633 nm) is focused through a 10 μm pin hole (PH). A 10-mm-diam iris (Iris 1) clips the resultant Airy pattern at its first null, and a lens (L2) collimates the beam to a diameter of approximately

25 mm. A 7-mm-diam iris (Iris 2) selects the center of the beam where aberrations are minimal. The beam next passes through an unpolarized 50/50 beam splitter which has a 0.5° wedge to avoid interference between the primary reflection and the weak reflection from the antireflection coated second surface. Iris 2 is imaged to the crystal face by a Newtonian telescope (L3 and L4) with unity magnification. This arrangement of lenses provides a well collimated beam at the crystal. The reflection from the crystal face is reimaged by the same telescope onto a 1 m focal length lens (L5) which, for a typical 5 mm×5 mm crystal, focuses the beam to a waist of approximately 100 μm at the detector. The lenses are all high quality 2-in.-diam achromats. The detector is an FND 100 large area silicon photodiode located 1 m from the focusing lens (L5). With this arrangement, a crystal tilt of 1 μrad results in a displacement of 1 μm at the detector.

The crystal is placed on a rotary encoder (Heidenhain ROD 553) that has an angular resolution of 1.75 μrad (0.0001°). The slits in front of the photodiode are typically set 10 μm apart, and we are able to measure the angle of the crystal faces to a precision of ±20 μrad. We first position the crystal to reflect from the input face to zero the rotary encoder, and then rotate the encoder and crystal to reflect from the output face. The precision of α is thus about ±40 μrad or $\pm0.002°$.

B. Measurement of βs

The indices of refraction, and from them the $\mathcal{N}$s, are determined by measuring the refraction angles β. They are measured using the apparatus shown in Fig. 4. The sample crystal is placed in a well collimated 1064 nm beam and tilted using a mirror mount so it precisely retroreflects the beam from its input face. A 532 nm detector placed on a swing arm is used to find the angles of the second harmonic beams. The pivot point of the arm is located at the point where the beams exit the crystal, but the crystal does not rotate. A rotary encoder (Heidenhain ROD 553) measures the angle of the arm. A 1 m focal length lens mounted on the swing arm focuses the harmonic light at the plane of the adjustable slits which are located 1 m downstream. To remove the fundamental light we insert both a dielectric mirror that has high reflectivity at 1064 nm and high transmission at 532 nm, and a KG3 colored glass filter, placed behind the slits, that absorbs the fundamental and passes the second harmonic. The zero angle of the swing arm is found by aligning the adjustable slits to the 1064 nm beam with the crystal removed, using the small amount of 1064 nm light that leaks through the 1064 nm reflector. Replacing the crystal in the beam, we measure the angles of the harmonic beams by rotating the swing arm while noting the angles of the harmonic beams. The harmonic light is detected using an RCA IP28 photomultiplier tube (PMT) biased at 1000 V. We make sure to keep the harmonic pulse energy within the linear range of the PMT. An opal glass diffuser immediately in front of the PMT spreads the light over the photocathode, minimizing any effects of local variations in sensitivity. We try to use the same point on the diffuser for all measurements. The β angles are typically measured with a precision of $\pm0.02°$

which, combined with the precision of α, yields refractive indices with a precision of one part in 10^4.

C. Pump light

The 1064 nm fundamental light is provided by a single-longitudinal-mode Nd:yttrium–aluminum–garnet (YAG) laser that produces 10 ns pulses full width half maximum at 10 pulses/s. We spatially filter the fundamental beam by focusing it through a 275-μm-diam diamond wire die (Indiana Wire Die). An iris (Iris 1) clips the resulting Airy pattern at its first null. We relay image the beam at Iris 1 onto the test crystal. Two polarizers and a half-wave plate (WP1) provide continuous adjustment of the pulse energy at the crystal. Another polarizer ensures a polarization purity greater than 99.95% at the crystal. After this polarizer a sapphire half-wave plate (Meller Optics) is used to vary the polarization angle ψ at the crystal. We use only sapphire wave plates rather than the more common quartz wave plates because quartz can generate a small amount of second harmonic but sapphire cannot due to its crystal symmetry.

Two reference detectors are used: one measuring harmonic light and one measuring fundamental light. The harmonic reference comprises a 50/50 beam splitter (BS1), an 8 mm long type II KTP crystal, and a 532 nm absorbing glass filter placed before the crystal to ensure that none of the 532 nm light generated in the KTP crystal is reflected back into the main beam path. A neutral density filter and a Galilean telescope are used to ensure that frequency doubling in the reference KTP crystal lies in the low conversion limit. The second harmonic reference light is detected by a vacuum photodiode (Hamamastu R1193U-01). An opal glass diffuser (not shown) and a 1064 nm absorbing glass filter are placed in front of the photodiode.

The fundamental reference uses an uncoated glass wedge to pick off part of the main beam for monitoring by a Hamamastu R1193U-01 vacuum photodiode. An opal glass diffuser in front of the photodiode spreads the light over its photocathode.

Whenever possible we normalize the signal pulse-by-pulse to the harmonic reference signal because this eliminates the influence of slight changes in the fundamental pulse shape. However, the fundamental reference has a larger dynamic range, so for crystals in which the free wave energies differ by 3 orders of magnitude or more, we must use the fundamental reference. Because the pulse-to-pulse energy stability of our laser is $\approx$1% rms, using the fundamental reference introduces errors of only $\approx$2%.

D. Optional elements

Optional optics are used at various stages in a measurement, but are typically not in the beam path during a measurement. While the crystal is being mounted, Iris 2 is narrowed to approximately 2 mm and the retroreflection from the crystal input face is centered on the iris. This makes it possible to align the crystal to $\pm$2 mrad.

A quarter-wave plate can be placed in the optical path after the half-wave plate to provide a $\pi/2$ phase difference between the vertically and horizontally polarized 1064 nm
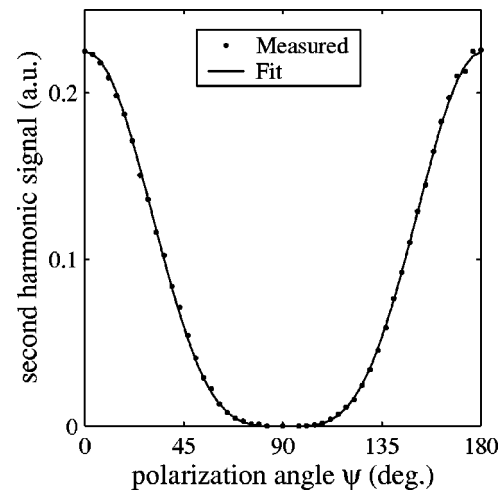

FIG. 5. Dependence of the z-polarized free wave on the polarization angle of the fundamental for the KDP reference crystal. The dots are measured values and the solid line is fit to the form $|A\cos^2(\psi_m+\epsilon)|^2$.

light. This changes the nature of the interference among the multiple contributing terms of Eq. (24) and may make analysis easier in certain situations. Perfect alignment of the wave plate requires that its slow and fast axes be exactly aligned with the crystal's eigenpolarizations. Any misalignment distorts the shape of the polarization dependence of the second harmonic. We found it difficult to precisely align the wave plate to the sample crystal, so we resorted to including a misalignment factor in our curve fitting routine. The quarter wave plate is also susceptible to etalon effects in which the reflectivity is slightly different for light polarized along the fast and slow axes. The antireflection coatings reduce surface reflections to 0.25%. However, the reflectivity anisotropy can still be as large as 1%. A 1% difference in fundamental power results in a 2% difference in the harmonic, which can be significant when the overall accuracy of the experiment is 2%.

The 532 nm half-wave plate positioned after the crystal was used to verify that the detection system is polarization insensitive. The polarizer positioned after the crystal is used to verify the polarization of the harmonic waves. It is removed during measurements of the harmonic signal strength and beam angles.

E. Data acquisition

We use a Camac based data acquisition system. The half-wave plate that rotates the polarization angle at the crystal (WP3) is typically rotated in increments of 0.9° or 1.8° using a computer controlled stepper motor (Slo-Syn). At each polarization angle we find a baseline signal by averaging ten laser pulses with the fundamental beam blocked by a shutter. We then average 50–100 pulses with the shutter open, subtracting the baselines and normalizing each signal pulse to the reference. The reference signals and the signal from the sample crystal are individually charge integrated on each pulse using box car gated integrators (SRS model SR250). No hardware averaging is performed. The box car outputs are digitized using 12 bit analog-to-digital converters. A

TABLE II. Multiplier $\mathcal{N}_{ijk}$ and its factors based on Sellmeier refractive indices for KDP with exit face tilted by $\alpha = 19.782°$, with the face normal lying in the $y - x$ plane.

Propagation direction (θ, ϕ)	Polarizations	$\dfrac{2k_0}{\Delta k}$	$t_1 t_1'$	t_2	$\dfrac{\bar{n}_1 + 1}{(n_2+1)(n_2+\bar{n}_1)}$	$\dfrac{2k_0(\bar{n}_1+1)t_1 t_1' t_2}{\Delta k (n_2+1)(n_2+\bar{n}_1)}\left[\dfrac{\cos\beta}{\cos\alpha}\right]^2$ $\mathcal{N}_{ijk}$
$(90°, 45°)$	$z - oo$	-42.7	0.6432	1.2292	0.3406	-11.03 ± 0.055

computer performs the normalization and averaging. Measurement of a typical curve of polarization dependence requires 10–30 min.

IV. KDP REFERENCE CRYSTAL

Measured values of d_{eff} for a sample crystal can be scaled to those of a reference crystal such as KDP by alternately placing the reference and sample crystals in the same experiment and measuring the relative second harmonic pulse energies. This eliminates the need for detailed characterization of the fundamental beam's spatial and temporal profiles as well as absolute calibrations of the input and output pulse energies. We use as a standard d_{zxy} of KDP which has a consensus value of 0.39 pm/V. Our KDP reference crystal is cut for propagation along the direction $(x = y)$, i.e., $(\theta = 90°, \phi = 45°)$. Its exit face is tilted with the face normal lying in the $x - y$ plane at a measured angle of $\alpha = 19.786°$.

A measurement of the z-polarized free wave generated by an $x - y$ polarized fundamental would be sufficient as a reference, but as a check on the cut of the reference crystal and of the purity of the fundamental polarization, we rotate the polarization angle of the linearly polarized fundamental 90° either side of the z orientation. The z-polarized free wave energy should obey

$$\mathcal{F}_z = CU_1^2 |d_{zxy}\mathcal{N}_{zxy}\cos^2\psi|^2 = A^2\cos^4(\psi_m + \epsilon), \quad (25)$$

where ψ is the polarization angle relative to the crystal lattice and ψ_m is the measured polarization angle. The variable ϵ is
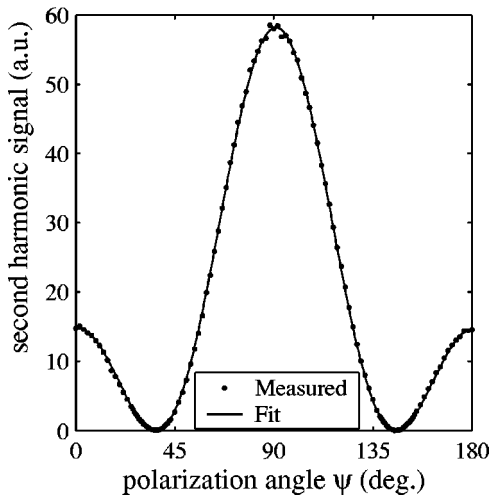

FIG. 6. Relative pulse energy of the x-polarized free wave from z-cut KNbO$_3$ as the polarization angle of the linearly polarized fundamental wave is rotated through 180°. At the left and right edges the fundamental is x polarized and at the center it is y polarized. The fit curve has the form shown in Eq. (27).

a small angle representing the difference between the laboratory and crystal lattice angles. Figure 5 shows the measured energy as dots along with a solid line fit to the data using the form of Eq. (25) with A and ϵ varied to obtain the best fit.

In order to use the KDP crystal as a reference it is necessary to know its value of $\mathcal{N}_{xxy}$. This calculation is outlined in Table II. The value of $\mathcal{N}_{zxy}$ was calculated using the refractive indices derived from the Sellmeier equation of Ghosh and Bhar.[12] The value calculated using the refractive indices deduced from our measured beam angles agrees within 1%.

V. KNBO$_3$ EXAMPLE

The form of the nonlinear tensor for KNbO$_3$, expressed in the optical frame in which $n_x < n_y < n_z$, is

$$\mathbf{d} = \begin{pmatrix} d_{xxx} & d_{xyy} & d_{xzz} & 0 & 0 & 0 \\ 0 & 0 & 0 & 0 & 0 & d_{yxy} \\ 0 & 0 & 0 & 0 & d_{zxz} & 0 \end{pmatrix}. \quad (26)$$

(Note that other axis systems are common in other reports.) Our KNbO$_3$ sample is cut for propagation along the z axis with the entrance face perpendicular to z and the exit face is tilted by $\alpha = 20.076°$ with its face normal lying in the $z - x$ plane. The x-polarized free wave energy is given by

$$\mathcal{F}_x = CU_1^2 |d_{xyy}\mathcal{N}_{xyy}\sin^2\psi + d_{xxx}\mathcal{N}_{xxx}\cos^2\psi|^2$$

$$= |R\sin^2(\psi_m + \epsilon) + S\cos^2(\psi_m + \epsilon)|^2. \quad (27)$$

Figure 6 shows the measured and fit curves of $\mathcal{F}_x$. The fit parameters are $S = 3.873$ and $R = -7.710$ in arbitrary units. Based on the measured β angle $\mathcal{N}_{xxx} = 1.598 \pm 0.019$ and $\mathcal{N}_{xyy} = -2.305 \pm 0.092$. This gives the ratio of tensor coefficients

$$d_{xxx}/d_{xyy} = 2.45. \quad (28)$$

Comparing the A fit coefficient for the KDP reference crystal with S and R for KNbO$_3$ gives $d_{xxx} = 21.9$ pm/V, $d_{xyy} = 8.93$ pm/V. Similar measurements of the y-polarized free wave returns the value of d_{yxy}. Substituting a y-cut crystal allows measurements of d_{xxx}, d_{xzz}, and d_{zxz}, completing the entire nonlinear tensor.[13]

VI. BIREFRINGENT CORRECTIONS

In some cases birefringence cannot be avoided. For example, in biaxial crystals it is necessary to propagate along directions other than the principal axes x, y, and z in order to measure the tensor elements d_{xyz}, d_{yxz}, and d_{zxy}. These elements are nonzero in biaxial crystals with point symmetry

1, 2, or 222. It is possible to measure these elements without walkoff of the free waves but with walkoff of the fundamental waves, so we examine the birefringence corrections to the theory presented above where lack of birefringence was assumed. There are two effects of fundamental wave walkoff. One is that the transmission coefficient t_1 changes. It becomes

$$t_1 = \frac{2}{(1+n_1)\cos\rho_1},\tag{29}$$

where ρ_1 is the walkoff angle for the fundamental wave. The second effect is that the fundamental electric field is tilted by ρ relative to the input face of the crystal. For propagation along $x = y$ ($\theta = 90°$, $\phi = 45°$) the Poynting vector tilt is toward the y axis, so $E_x = E_1 \sin(45° + \rho_1)$ and $E_y = E_1 \cos(45° + \rho_1)$ and E_x and E_y are not equal. Similar considerations apply to propagation in the other two principal planes.

Although it is never necessary to use a crystal cut so the free wave has birefringent walkoff, it may be convenient to do so. This free wave walkoff also has two effects, one being a change in the transmission coefficient for a p-polarized free wave at the exit face. It becomes

$$t_2 = \frac{n_r \cos\rho_r \cos(a \pm |\rho_2|) + n_2 \cos\rho_2 \cos(\sigma \pm |\rho_r|)}{n_r \cos\rho_r \cos\beta + \cos(\sigma \pm |\rho_r|)},\tag{30}$$

where ρ_2 is the walkoff angle of the free wave, and the signs used for the $\pm$ depend on whether walkoff increases or decreases the angles between the Poynting vectors of the free and reflected waves and the exit face normal. The other effect is to change the expression for the driven wave, and by implication the expression for the free wave as well. For propagation in the $x - y$ plane the (xy)-polarized driven wave is[5,14]

$$E_d = \frac{-n_2^2}{(n_2^2 - \bar{n}_1^2)}\left[\boldsymbol{\epsilon}^{-1}\!:\!P_{\mathrm{NL}} - \frac{\bar{n}_1^2}{n_x^2 n_y^2}\hat{k}(\hat{k}\cdot P_{\mathrm{NL}})\right],\tag{31}$$

where

$$\boldsymbol{\epsilon}^{-1} = \frac{1}{\epsilon_0}\begin{pmatrix} n_x^{-2} & 0 \\ 0 & n_y^{-2} \end{pmatrix}\tag{32}$$

and $n_x(n_y)$ is the refractive index for a harmonic wave whose electric field is parallel to the $x(y)$ axis. The second term in the brackets of Eq. (31) lies along the propagation direction and so does not contribute to the tangential compo-

nent of the driven wave at the input face, assuming normal incidence. Applying the boundary conditions of continuous tangential electric and magnetic fields for propagation along direction ($\theta = 90°$, ϕ) gives

$$E_f = \hat{e}_f \frac{P_{\mathrm{NL}}\cdot\hat{e}_f}{\epsilon_0(n_2^2 - \bar{n}_1^2)}\left[\frac{\bar{n}_1 + 1}{n_2 + 1}\right]n_2^4\left[\frac{\sin^2\phi}{n_x^4} + \frac{\cos^2\phi}{n_y^4}\right],\tag{33}$$

where $\hat{e}_f$ is a unit vector along the direction of the free wave electric field. It is tilted by the walkoff angle ρ_2 from the crystal input face. Using the usual definition of d_{eff} and taking account of the actual field directions this becomes

$$\begin{aligned} E_f &= \hat{e}_f \frac{d_{\mathrm{eff}}}{(n_2^2 - \bar{n}_1^2)}\left[\frac{\bar{n}_1 + 1}{n_2 + 1}\right]n_2^4\left[\frac{\sin^2\phi}{n_x^4} + \frac{\cos^2\phi}{n_y^4}\right] \\ &= \hat{e}_f \frac{d_{\mathrm{eff}}}{(n_2^2 - \bar{n}_1^2)}\left[\frac{\bar{n}_1 + 1}{n_2 + 1}\right]\left[\frac{1}{\cos\rho_2}\right]^2 \end{aligned}\tag{34}$$

and the modified $\mathcal{N}$ is

$$\mathcal{N} = \frac{2k_0 t_1 t_1' t_2}{\Delta k(n_2 + \bar{n}_1)}\left[\frac{\bar{n}_1 + 1}{n_2 + 1}\right]\left[\frac{1}{\cos\rho_2}\right]^2\left[\frac{\cos\beta}{\cos(\alpha + \rho_2)}\right]^{1/2}.\tag{35}$$

ACKNOWLEDGMENTS

[1] P. A. Franken, A. E. Hill, C. W. Peters, and G. Weinreich, Phys. Rev. Lett. **7**, 118 (1961).
[2] R. J. Gehr and A. V. Smith, J. Opt. Soc. Am. B **15**, 2298 (1998).
[3] P. D. Maker, R. W. Terhune, M. Nisenoff, and C. M. Savage, Phys. Rev. Lett. **8**, 21 (1962).
[4] I. Shoji, T. Kondo, A. Kitamoto, M. Shirane, and R. Ito, J. Opt. Soc. Am. B **14**, 2268 (1997).
[5] W. N. Herman and L. M. Hayden, J. Opt. Soc. Am. B **12**, 416 (1995).
[6] R. Morita, T. Kondo, Y. Kaneda, A. Sugihashi, N. Ogasawara, S. Umegaki, and R. Ito, Jpn. J. Appl. Phys., Part 2 **27**, L1134 (1998).
[7] J. Jerphagnon and S. K. Kurtz, J. Appl. Phys. **41**, 1667 (1970).
[8] D. Chemla and P. Kupecek, Rev. Phys. Appl. **6**, 31 (1970).
[9] M. M. Choy and R. L. Byer, Phys. Rev. B **14**, 1693 (1976).
[10] I. Shoji, T. Kondo, and R. Ito, Opt. Quantum Electron. **34**, 797 (2002).
[11] N. Bloembergen and P. S. Pershan, Phys. Rev. **128**, 606 (1962).
[12] G. C. Ghosh and G. C. Bhar, IEEE J. Quantum Electron. **QE-18**, 143 (1982).
[13] M. V. Pack, D. J. Armstrong, and A. V. Smith, J. Opt. Soc. Am. B (to be published).
[14] N. Okamoto, Y. Hirano, and O. Sugihara, J. Opt. Soc. Am. B **9**, 2083 (1992).